Low-Energy Neutron Scattering by a Spheroidal Complex Potential*

B. MARGOLIS AND E. S. TROUBETZKOY
Physics Department, Columbia University, New York, New York
(Received December 21, 1956)

The scattering and absorption of low-energy neutrons ($kR \ll 1$) by complex square well potentials of spheroidal shape $r=R(1+aP_2)$ is calculated by expanding the neutron wave function in terms of appropriate spherical Bessel and Neumann functions times spherical harmonics. The convergence of the results obtained is demonstrated.

The "strength function" $\bar{\Gamma}_n^0/D$, the average value of neutron width to spacing, is of particular interest in nuclear physics. It can be calculated from the scattering amplitude.

This strength function is plotted as a function of atomic number in the region $A>90$. The results are seen to deviate considerably from the corresponding results for spherical nuclei. Comparison is made with experiment.

INTRODUCTION

COMPLEX potentials have been used extensively in the past few years[1,2] in interpreting neutron reaction cross-section measurements. At low energies (<3 Mev) the experimental data are best fitted with a potential in which the imaginary part is only a few percent of the real part.

If one goes low enough in energy experimentally, one sees the high, narrow Breit-Wigner resonances corresponding to discrete compound states. The complex potential leads to cross sections which should be interpreted only as averages over these fine structure resonances. Plotting these average cross sections against energy and atomic number, one still finds resonant structure, the so-called "shape resonances." Of particular interest in this low-energy region is the strength function, the average value of neutron width divided by the average level spacing for a given nucleus, normalized to some energy (1 ev here) and plotted against atomic number. This relates to the average absorption cross section through formula (9b).

Experimental data obtained by two different methods have been plotted in Figs. 5 and 6. One method[3] involves measurement of discrete resonances. The other[4] involves the measurement of cross sections in the kev region where the experimental resolution is much worse than the level spacing. Here, then, measurements of cross section should give results that agree with the cross sections calculated using a complex potential. The strength function is then determined through formula (9b).

The resonant structure of the strength function has been discussed by Bohr and Mottelson,[5] Feshbach, Porter, and Weisskopf,[2] Weisskopf,[6] and Lane, Thomas, and Wigner.[7] Feshbach, Porter, and Weisskopf[2] have calculated the strength function using a complex square well of spherical shape.

Nuclear shapes are known to be deformed from the spherical away from closed shells.[8] This suggests it might be more realistic to use a complex potential of nonspherical shape in discussing neutron scattering from these nuclei. In particular, in this paper we have considered deviations from spherical shape of a quadrupole character. These shapes are called spheroidal here. We consider particularly the heavier nuclei, $A>90$. A nucleus with a quadrupole moment has nonzero angular momentum and the symmetry axis if the nucleus (assuming that there is one) precesses about the fixed angular momentum vector. This precession, however, is slow compared to the period of motion of the neutrons in a well of depth of the order of 40 Mev as long as the quadrupole moment is not too small; i.e., away from closed shells.[3] It is realistic then to consider scattering by a static potential of spheroidal shape.

The purpose of this paper is to demonstrate the modifications in low-energy neutron scattering that occur when the potential has a spheroidal rather than a spherical shape. Deformations of shape other than the quadrupole can be treated by methods similar to those used below. The methods used here are applicable to other problems of scattering from spheroids where the wavelength is much larger than the dimensions of the scatterer.

SCATTERING BY SPHERICAL COMPLEX POTENTIAL

The wave function for s-wave neutrons scattered by complex potential

$$\begin{aligned} V&=-V_0(1+i\zeta), \quad r<R \\ &=0, \qquad\qquad r<R \end{aligned} \tag{1}$$

* This work was partially supported by the U. S. Atomic Energy Commission.

[1] H. A. Bethe, Phys. Rev. **57**, 1125 (1940).
[2] Feshbach, Porter, and Weisskopf, Phys. Rev. **96**, 448 (1954).
[3] Harvey, Hughes, Carter, and Pilcher, Phys. Rev. **99**, 10 (1955).
[4] Schwartz, Pilcher, Hughes, and Zimmerman, Bull Am. Phys. Soc. Ser II, **1**, 347 (1956).
[5] A. Bohr and B. R. Mottelson, Kgl. Danske Videnskab. Selskab, Mat.-fys. Medd **27**, 16 (1953).
[6] V. F. Weisskopf in *Proceedings of International Conference on the Peaceful Uses of Atomic Energy, Geneva, August, 1955* (United Nations, New York, 1956), Vol. 2.
[7] Lane, Thomas, and Wigner, Phys. Rev. **98**, 693 (1955).
[8] Townes, Foley, and Low, Phys. Rev. **76**, 1415 (1949).

in the region $r>R$ is given by

$$y=\frac{i}{2kr}(e^{-ikr}-\bar{\eta}_0 e^{ikr}), \tag{2}$$

where

$$\bar{\eta}_0=e^{-2ix}\left(\frac{X\cot X+ix}{X\cot X-ix}\right). \tag{3}$$

In the above equation, $x=kR$, where k is the wave number of the incident neutrons and $X^2=x^2+(2M/\hbar^2)\times V_0(1+i\zeta)R^2\equiv K^2R^2$.

At low enough energies where the Breit-Wigner-type resonances are well spaced, $\bar{\eta}_0$ can be considered as an average over the neutron resonance scattering amplitudes given by[2]

$$\eta_0=e^{-2ikR'}\left(1-\frac{i\Gamma_n{}^s}{E-E_s+i\Gamma^s/2}\right)+\eta_0{}^*, \tag{4}$$

where $\Gamma_n{}^s$, Γ^s are the neutron and total widths of the compound nucleus level of energy E_s, R' is a length of the order of nuclear dimensions, E is the incident neutron energy, and $\eta_0{}^*$ is the contribution of levels other than that at energy E_s as well as interference of the sth level with the other levels. Feshbach, Porter, and Weisskopf[2] show that $\eta_0{}^*$ contributes a negligible amount to the average of η_0 if the spacing of the levels is much larger than the level widths. Averaging η_0 over resonances yields

$$\bar{\eta}_0=e^{-2ikR'}(1-\pi\bar{\Gamma}_n/D), \tag{5}$$

where D is the average spacing of the levels and $\bar{\Gamma}_n$ is the average value of the neutron widths. It follows that, for $kR'\ll 1$,

$$\bar{\Gamma}_n/D=(1/\pi)\,\mathrm{Re}(1-\bar{\eta}_0), \tag{6}$$

$$kR'=\tfrac{1}{2}\,\mathrm{Im}(1-\bar{\eta}_0). \tag{7}$$

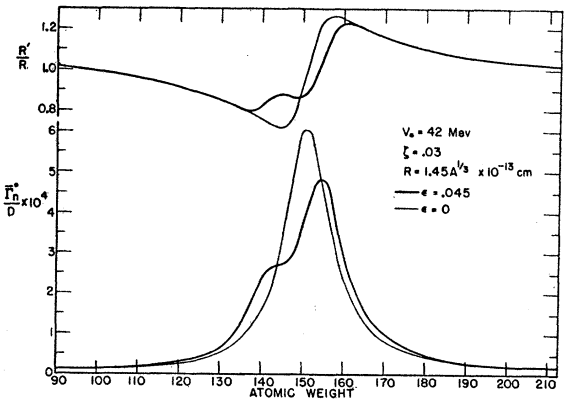

FIG. 1. Effective radius R' and the ratio $\bar{\Gamma}_n{}^0/D$ of average neutron width to the average level spacing as a function of A. The strength function $\bar{\Gamma}_n{}^0/D$ is normalized to 1 ev, and R' is plotted in units of R. The curves correspond to a spherical nucleus, and to spheroidal nuclei with eccentricity $\epsilon=0.045$.

The strength function and R' can be evaluated using the form (3) for $\bar{\eta}_0$. Equation (3) can be written for $x\ll 1$ in the form

$$1-\bar{\eta}_0=ix\left(1-\frac{1}{X\cot X}\right). \tag{8}$$

The average scattering and absorption cross sections using average scattering amplitudes are given by the usual expressions:

$$\bar{\sigma}_{sc}=\frac{\pi}{k^2}|1-\bar{\eta}_0|^2\simeq 4\pi R^2, \tag{9a}$$

$$\bar{\sigma}_a=\frac{\pi}{k^2}(1-|\bar{\eta}_0|^2)\simeq\frac{2\pi^2\,\bar{\Gamma}_n}{k^2\;D}. \tag{9b}$$

The equalities on the right-hand side are valid in the low-energy region of well-spaced levels. Here $\bar{\sigma}_{sc}$ refers to potential elastic scattering and $\bar{\sigma}_a$ to compound nucleus formation. For low energies, if the (n,γ) process is negligible, only elastic scattering contributes to $\bar{\sigma}_a$.

SCATTERING BY SPHEROIDAL POTENTIAL

If the complex potential has a spheroidal boundary, a solution of the following Schrödinger equation is desired.[9]

$$\nabla^2\psi+(k^2-V)\psi=0,$$
$$U=0,\quad r>R[1+aP_2(\cos\theta)]=-(2M/\hbar^2)V_0(1+i\zeta),$$
$$r<R[1+aP_2(\cos\theta)]. \tag{10}$$

The form $r=R(1+aP_2)$ for the boundary of the square well puts the axis of symmetry of the spheroid along the z axis. Since very low-energy scattering is considered here, only *ingoing* waves of angular momentum zero are important. It will be seen that asymptotically there will be only s-state outgoing waves too. We are free then to choose the axis of symmetry as we please. The low-energy scattering will be independent of the spheroid orientation. In terms of the spheroid axes lengths b and c, c being the length of the symmetry axis.

$$\tfrac{3}{2}a\simeq\epsilon\equiv(c^2-b^2)/(c^2+b^2), \tag{11}$$

where ϵ is defined as the eccentricity of the spheroid. The approximation $a=\frac{2}{3}\epsilon$ is a good one for $a\lesssim 0.1$.

Solutions of (10) for the outside and inside regions can be written in the form

$$\psi_O=\sum(2l+1)i^l\tfrac{1}{2}[h_l{}^{(2)}(kr)+\eta_l h_l{}^{(1)}(kr)]P_l(\cos\theta)$$
$$=\sum(2l+1)i^l[j_l(kr)+\tfrac{1}{2}(\eta_l-1)h_l{}^{(1)}(kr)]P_l(\cos\theta),$$
$$r>R(1+aP_2) \tag{12a}$$

$$\psi_I=\sum A_l j_l(Kr)P_l(\cos\theta),\quad r<R(1+aP_2) \tag{12b}$$

where the outside wave function has been normalized so the incident plane wave is given by e^{ikz}. j_l are spher-

[9] It is to be noted that the wave equation (10) does not separate in any system of coordinates.

ical Bessel functions and h_l spherical Hankel functions of the first and second kind.

It remains to join the inside and outside region wave functions and their derivatives at the surface of the well. In the case of a spherical well, angular momentum is a good quantum number and one merely equates coefficients of P_l. This determines the η_l and A_l. In the case of a spheroidal scatterer, angular momentum is not a good quantum number and we must write

$$\sum_{l=0,2}^{\infty} A_l j_l(Y) P_l = \sum_{l=0,2}^{\infty} (2l+1) i^l \times [j_l(y) + \tfrac{1}{2}(\eta_l - 1) \cdot h_l^{(1)}(y)] P_l, \quad (13a)$$

where $Y = X[1+aP_2(\cos\theta)]$ and $y = x[1+aP_2(\cos\theta)]$. The sums are taken only over even l values since parity is a good quantum number. Since for $x \ll 1$ only $l=0$

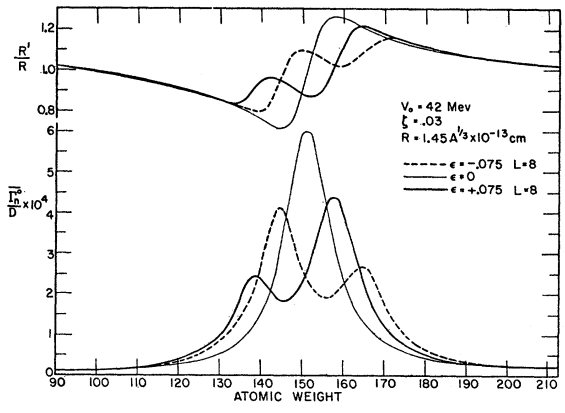

FIG. 2. Effective radius R' and the ratio $\bar{\Gamma}_n^0/D$ of average neutron width to the average level spacing as a function of A. The strength function $\bar{\Gamma}_n^0/D$ is normalized to 1 ev, and R' is plotted in units of R. The curves correspond to a spherical nucleus, and to spheroidal nuclei with eccentricities $\epsilon = \pm 0.075$.

ingoing waves are important it follows that all odd l waves are unscattered. Another equation can be written for the radial derivatives of the inside and outside wave functions at $R(1+aP_2)$:

$$\frac{\partial}{\partial r}\psi_I = \frac{\partial}{\partial r}\psi_O. \quad (13b)$$

Equations (13) must then be made to hold for all values of θ. Since the series (12) for ψ are formed from complete sets it should be possible to solve for the A_l and η_l. It is instructive to multiply both sides of Eqs. (13) by $P_l(\cos\theta)$ and integrate from $\theta=0$ to 2π for $l=0, 2, 4, \cdots$. One then finds readily for even l (see Appendix I) the approximate proportionalities:

$$A_l \propto a^{l/2}[1+O(a)] \quad \text{as} \quad x \to 0 \quad (14)$$

and

$$\eta_l - 1 \propto a^{l/2}[1+O(a)]x^{l+1} \quad \text{as} \quad x \to 0. \quad (15)$$

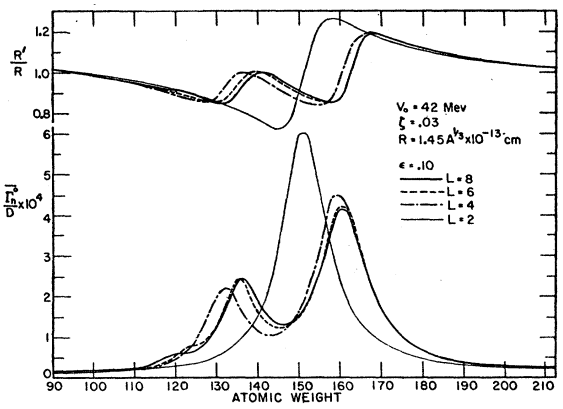

FIG. 3. Effective radius R' and strength function $\bar{\Gamma}_n^0/D$ as a function of A for a spheroidal nucleus of eccentricity $\epsilon=0.1$. The curves represent the calculations in approximations of successive order. The $L=2$ approximation yields the results for spherical nuclei and the successive order approximations give information on the convergence of the calculations. $L=8$ for example represents the calculation in which inside and outside wave functions and their derivatives were joined at angular positions given by the roots of $P_8(\mu)=0$.

It is important to note that for a spherical square well one has approximately

$$\eta_l - 1 \propto x^{2l+1} \quad \text{as} \quad x \to 0. \quad (15a)$$

Relations (14) and (15) show that for x and $a \ll 1$ only a few values of l will contribute appreciably to the expressions (13). A comparison of relations (15) and (15a) shows why even for low energies it is important to include terms for $l>0$ in the scattered wave in the case of a spheroidal potential whereas for a spherical potential they are negligible. For $l>0$, $r=R$, the lth partial wave of Eq. (12a) has the approximate form

$$u_l \propto a^{l/2} x^{l+1} \eta_l(kR) \propto a^{l/2}, \quad (16)$$

whereas for the case of a spherical potential it has the approximate form

$$v_l \propto x^{2l+1} \eta_l(kR) \propto x^l \to 0. \quad (16a)$$

However, as $r \to \infty$, as in the spherical case,

$$\psi \to \frac{e^{-ikr} - \eta_0 e^{ikr}}{-2ikr}. \quad (17)$$

Equations (13) can be made to yield η_0 as follows. Neglect values higher than $l=L$, say. Put $\cos\theta = \mu_i$, $i=1, 2, 3, \cdots, L/2$, where μ_i are the roots of $P_L(\mu)=0$. One then has L linear equations in the L unknowns A_l and $(1/x^{l+1})(\eta_l - 1)$, $l=0, 2, 4, \cdots, L-2$. These can be solved for η_0, which then yields the strength function and R' through Eqs. (6) and (7) which carry over to the case of spheroidal nuclei.

RESULTS AND CONCLUSIONS

In practice, solving Eqs. (13) is a tedious, difficult business since several l values are required to obtain

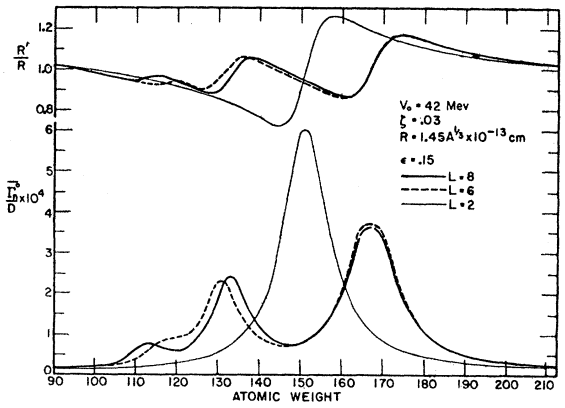

FIG. 4. Effective radius R' and strength function $\bar{\Gamma}_n^0/D$ as a function of A for a spheroidal nucleus of eccentricity $\epsilon=0.15$, and for a spherical nucleus. Calculations in approximations of the two highest orders considered are plotted.

convergence for eccentricities such as occur in nuclear shapes. It was found profitable to program the calculation for a computing machine. Figures 1 to 4 show $\bar{\Gamma}_n^0/D$ and R'/R for spheroidal nuclei plotted against atomic number in the range of atomic numbers $A=90$ to 210 for eccentricities $\epsilon=0.045$, 0.075, 0.1, 0.15, and -0.075. The corresponding curves for spherical nuclei are also plotted. In all cases $V_0=42$ Mev, $\zeta=0.03$ and $R=1.45\times A^{\frac{1}{3}}\times 10^{-13}$ cm. $\bar{\Gamma}_n^0$ refers to $\bar{\Gamma}_n$ normalized to an energy $E=1$ ev.

For eccentricites $\epsilon=\pm 0.075$ and $\epsilon=0.045$, the curves of the strength function and R' when one takes $L=6$ almost coincide at all points with those when $L=8$. The curves plotted in Figs. 1 and 2 were obtained by taking $L=8$ and represent convergent results.

Figure 3 shows results for $\epsilon=0.1$ taking $L=2$, 4, 6, 8 ($L=2$ corresponds to the spherical result). The necessity of taking higher l values into account for larger eccentricities is clearly demonstrated. It was decided to stop at $L=8$ because of the amount of calculation involved. The third maximum, which starts to show up for $\epsilon=0.1$, appears more definitely in Fig. 4 ($\epsilon=0.15$). The maxima can be understood in terms of spherical potential results as follows. For scattering by spherical square well potentials, the scattering amplitude for angular momentum l is given by[2]

$$\eta_l=e^{-2i\delta_l}\left(1+\frac{2iS_l}{[1+Xj_l'(X)/j_l(X)]-\Delta_l+iS_l}\right), \quad (18)$$

where

$$\Delta_l+iS_l=1+xh_l^{(1)\prime}(x)/h_l^{(1)}(x),$$
$$\delta_l=\tan^{-1}[-j_l(x)/n_l(x)].$$

One then has resonances in the cross section when the real part of the denominator on the right side of (18) vanishes. For low energies, i.e., as $x\to 0$, this condition becomes

$$X_R j_l'(X_R)+(l+1)j_l(X_R)=0. \quad (19)$$

For $l>0$, this is equivalent to $j_{l-1}(X_R)=0$. In the above equation, X_R is the real part of X. The small changes due to the small imaginary part of X are neglected.

The nonspherical part of the potential in (10) acts to mix these resonances since for such a potential angular momentum is not a good quantum number. At low energies for spherical scattering centers only the $l=0$ resonances are excited. Because of the mixing of angular momenta for nonspherical scatterers, this is not the case for the latter. One has solutions of (19) for $l=0$ at $X_R=11$ ($A=151$) for $l=2$ at $X_R=10.9$ ($A=147$) and $l=4$ at $X_R=10.4$ ($A=128$). The $l=0$ and 2 resonances, because of their small separation, mix strongly and this accounts for the two peaks in $\bar{\Gamma}_n^0/D$ in Fig. 2.

Increasing the nonspherical part of the potential by increasing the eccentricity ϵ increases the splitting in the resonance positions. This is much as one finds in the splitting of degenerate or near degenerate states by a perturbing potential in bound state problems. For higher eccentricities, the coupling to other l resonances becomes significant as is seen in Figs. 3 and 4.

The experimental strength functions[3,4] (Fig. 5) in the region $A=155$ to 188, where nuclear deformations are comparatively large, agree much better on the whole with the spheroidal well values than with the spherical. It is indeed possible to fit the experimental strength functions in this region by using eccentricities of magnitude $\epsilon\lesssim 0.2$.

On the other hand, the strength functions for nuclei with neutron number near the closed shell $N=82$ (see Fig. 6) have strength functions which agree very well with the spherical well calculated curve. Data are lacking near $Z=82$, $A=126$ to make a similar comparison.

For $A\sim 230$ to 240, the measured strength functions are considerably higher than those calculated using a spherical well. In this region, for reasonable eccentricities, the spheriodal well results do not deviate from the spherical. These high strength functions could be explained by mixing with odd-l spherical potential

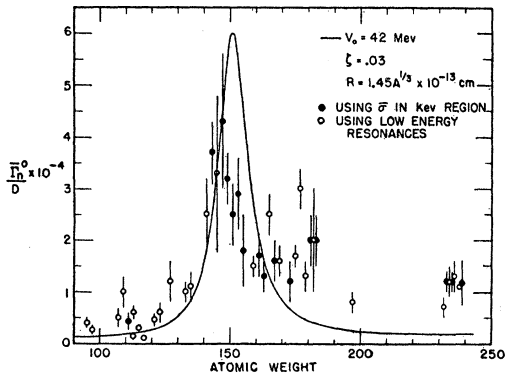

FIG. 5. Experimental values[3,4] of the strength function $\bar{\Gamma}_n^0/D$. The curve is the theoretical strength function for a spherical nucleus.

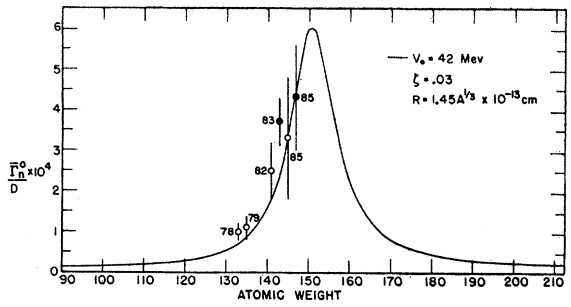

FIG. 6. Experimental values of the strength function $\bar{\Gamma}_n^0/D$ for nuclei near closed shells. The number of nucleons approaching a magic number has been written beside each experimental point. The curve is the theoretical strength function for a spherical potential.

resonances. Solutions of (19) with angular momentum $l=1,3$ exist in this region of atomic number for a well of 42-Mev depth. To excite odd-l resonances requires a well with a shape depending on odd harmonics. Evidence for shapes of this type comes from the fact that there are low-lying 1− states for even-even nuclei in this region of A.[10] The character of these states suggests that they may be rotational states. This would make for nuclear deformations of odd spherical harmonic shape.

ACKNOWLEDGMENTS

We wish to thank Watson Scientific Computing Laboratories for the use of their computing machine I.B.M. type 650.

APPENDIX I

Equations (13) for fitting the inside and outside wave functions at the boundary $r=R[1+aP_2(\cos\theta)]$ are identities with respect to θ, and have to be solved for the A_l's and η_l's. If one takes successive moments of these equations by multiplying by P_l and integrating over θ, one obtains as many independent equations as needed.[11]

For the sake of simplicity, let us cut off Eqs. (13) at $l=2$ and take the first two moments. Keeping terms up to the order of a^2, we get for $x\ll 1$

$$\left[j_0+\frac{(aX)^2}{10}j_0''\right]A_0+\frac{aX}{5}\left[j_2'+\frac{aX}{7}j_2''\right]A_2 +i\left(1+\frac{a^2}{5}\right)\frac{(\eta_0-1)}{2x^3}+i9a\frac{(\eta_2-1)}{2x^3}=1, \quad \text{(A1a)}$$

$$\left[Xj_0'+\frac{P^2}{10}(Xj_0')''\right]A_0+\frac{aX}{5}\left[(Xj_2')'+\frac{ax}{7}(Xj_2')''\right]A_2 -i\left(1+\frac{2a^2}{5}\right)\frac{(\eta_0-1)}{2x}-27ai\frac{(\eta_2-1)}{2x^3}=0, \quad \text{(A1b)}$$

$$aX\left[j_0'+\frac{aX}{7}j_0''\right]A_0+\left[j_2+\frac{2}{7}(aX)j_2'+\frac{3}{14}(aX)^2j_2''\right]A_2 -ia\frac{(\eta_0-1)}{2x}-15i\frac{(\eta_2-1)}{2x^3}=0, \quad \text{(A2a)}$$

$$aX\left[(Xj_0')'+\frac{aX}{8}(Xj_0')''\right]A_0 +\left[Xj_2'+\frac{2}{7}(aX)(Xj_2')'+\frac{3}{14}aX^2(Xj_2')''\right]A_2 +ai\frac{(\eta_0-1)}{2x}+45i\frac{(\eta_2-1)}{2x^3}=0, \quad \text{(A2b)}$$

where Eqs. (A1) and (A2) correspond to the zeroth and second moments respectively, and Eqs. (a) and (b) come from (13a) and (13b) respectively. The primes denote derivatives with respect to X, the argument of the Bessel functions.

Inspecting Eqs. (A2), one sees that to the lowest order in a:

$$A_2\propto a,$$
$$\eta_2-1\propto ax^3.$$

More generally, taking into account higher l values, one has

$$A\propto a^{l/2};\quad \eta_l-1\propto a^{l/2}x^{l+1}.$$

[10] Stephens, Asaro, and Perlman, Phys. Rev. **100**, 1543 (1955).

[11] This is not the procedure that was used to solve for η_0 in the machine calculation. That procedure was described earlier.